Range-wide variation in local adaptation and phenotypic plasticity of fitness-related traits in Fagus sylvatica and their implications under climate change

Homero Alejandro Gárate-escamilla, Arndt Hampe, Natalia Vizcaíno-palomar, T. Matthew Robson, Marta Benito-Garzón

HAL Id: hal-02625802
https://hal.inrae.fr/hal-02625802

Submitted on 3 Jun 2024

Range-wide variation in local adaptation and phenotypic plasticity of fitness-related traits in *Fagus sylvatica* and their implications under climate change

Homero Gárate-Escamilla[1], Arndt Hampe[1], Natalia Vizcaíno-Palomar[1], T. Matthew Robson[2] & Marta Benito Garzón[1*].

[1]BIOGECO INRA UMR 1202 University of Bordeaux, Pessac, 33400, France

[2] Organismal and Evolutionary Biology (OEB), Viikki Plant Science Centre (ViPS), Faculty of Biological and Environmental Sciences, University of Helsinki, P.O. Box 65, Finland 00014.

*Corresponding author: marta.benito-garzon@inra.fr

ACKNOWLEDGEMENTS

BIOSKETCH

The authors' research is focused on plant ecology and global change. The authors use multidisciplinary approaches including ecophysiology, genetics and ecological modelling to understand complex processes in ecology at large geographical scales.

22   **Running title:** range-wide multi-trait variation

23   **Keywords**: phenotypic variation, species distribution models, beech, acclimation, trait co-

24   variation, common gardens

25

26

27   **ABSTRACT**

28   **Aim:** To better understand and more realistically predict future species distribution ranges, it is

29   critical to account for local adaptation and phenotypic plasticity in populations' responses to

30   climate. This is challenging because local adaptation and phenotypic plasticity are trait-

31   dependent and traits co-vary along climatic gradients, with differential consequences for fitness.

32   Our aim is to quantify local adaptation and phenotypic plasticity of vertical and radial growth,

33   leaf flushing and survival across *Fagus sylvatica* range and to estimate each trait contribution to

34   explain the species occurrence.

35   **Location:** Europe

36   **Time period:** 1995 – 2014; 2070

37   **Major taxa studied:** *Fagus sylvatica L.*

38   **Methods:** We used vertical and radial growth, flushing phenology and mortality of *Fagus*

39   *sylvatica* L. recorded in BeechCOSTe52 (>150,000 trees). Firstly, we performed linear mixed-

40   effect models that related trait variation and co-variation to local adaptation (related to the

41   planted populations' climatic origin) and phenotypic plasticity (accounting for the climate of the

42   plantation), and we made spatial predictions under current and RCP 8.5 climates. Secondly, we

43   combined spatial trait predictions in a linear model to explain the occurrence of the species.

44   **Results:** The contribution of plasticity to intra-specific trait variation is always higher than that

45   of local adaptation, suggesting that the species is less sensitive to climate change than expected;

46   different traits constrain beech's distribution in different parts of its range: the northernmost edge

47   is mainly delimited by flushing phenology (mostly driven by photoperiod and temperature), the

48   southern edge by mortality (mainly driven by intolerance to drought), and the eastern edge is

49   characterised by decreasing radial growth (mainly shaped by precipitation-related variables in

50   our model); considering trait co-variation improved single-trait predictions.

51   **Main conclusions:** Population responses to climate across large geographical gradients are trait-

52   dependent, indicating that multi-trait combinations are needed to understand species' sensitivity

53   to climate change and its variation across distribution ranges.

54

55

56

57

58

59

60

61

62

63

64

65

66

67

68

69 **1. INTRODUCTION**

70 Climate change is having a major impact on the structure, composition and distribution of forests

71 worldwide (Trumbore, Brando, & Hartmann, 2015). Accordingly, numerous models have

72 projected significant range shifts of forest tree species towards higher latitudes and elevations

73 (Urban et al., 2016). However, to date, the two most important processes in the response of tree

74 populations to a rapidly changing climate, local adaptation and phenotypic plasticity (Aitken,

75 Yeaman, Holliday, Wang, & Curtis-Mclane, 2008; Savolainen, Pyhäjärvi, & Knürr, 2007), are

76 not systematically considered by species distribution models (but see Duputié, Rutschmann,

77 Ronce, & Chuine, 2015; Richardson, Chaney, Shaw, & Still, 2017; Valladares et al., 2014).

78 Phenotypic plasticity enables a given genotype to express different phenotypes in response to

79 changing environments, while local adaptation produces new genotypes with a greater ability to

80 cope with the new environment. The two mechanisms are ubiquitous in natural populations,

81 although their respective importance is considered to vary extensively through time and across

82 species ranges (Des Roches et al., 2018; Reich et al., 2016). To better understand and more

83 realistically predict future species distribution ranges, it is therefore critical to identify and

84 quantify the respective importance of local adaptation and phenotypic plasticity in the response

85 of local populations to a changing climate.

86   From an ecological perspective, fitness can be associated with several phenotypic traits

87 which directly affect survival and reproduction, creating a fitness landscape (Laughlin, 2018)

88 that allows them to be used to bound species ranges (Benito-Garzón, Ruiz-Benito, & Zavala,

89 2013; Stahl, Reu, & Wirth, 2014). Fitness-related traits vary across large geographical gradients,

90 mainly depending on how natural selection drove differences among populations in the past. For

91 instance, tree height is generally greatest at the core of a species range and decreases towards its

92   margins (Pedlar & McKenney, 2017). Climate-driven mortality commonly increases towards the

93   driest part of a species range, which is related to drought-induced stress conditions (Benito

94   Garzón et al., 2018). The onset of flushing phenology tends to be delayed towards high latitudes

95   (Duputié et al., 2015) as a consequence of genetic adaptation to late frost and fluctuating

96   photoperiod (Way & Montgomery, 2015). Moreover, traits tend to co-vary across climatic

97   gradients (Laughlin & Messier, 2015). A conspicuous example is the demographic compensation

98   found between survival and growth near range margins (Benito-Garzón et al., 2013; Doak &

99   Morris, 2010; Peterson, Doak, & Morris, 2018). New climatic conditions can result in

100 maladaptation of some populations, which may change intra-specific patterns of trait variation

101 and co-variation across geographical gradients, and eventually, species ranges. For example,

102 increasing temperatures at high-latitude or high-elevation range margins are likely to produce

103 higher growth rates, but they can also induce higher mortality owing to late frosts (Delpierre,

104 Guillemot, Dufrêne, Cecchini, & Nicolas, 2017; Vitasse, Lenz, Hoch, & Korner, 2014). Hence,

105 species ranges are likely to be delimited by the interaction of multiple traits and their responses

106 across environmental gradients (Benito-Garzón et al., 2013; Enquist et al., 2015; Stahl et al.,

107 2014).

108   Common gardens or provenance tests provide us with the necessary experiments to

109 quantify phenotypic plasticity and local adaptation of fitness-related traits in response to climate

110 (Mátyás, 1999). Models based on reaction norms of phenotypic traits using measurements

111 recorded in common gardens show that: (i) geographic variation in populations' responses to

112 climate is more strongly based on phenotypic plasticity than on local (Benito Garzón, Robson &

113 Hampe, *Under Review*); (ii) phenotypic variation can strongly differ among traits, in particular

114 for tree survival, growth, and flushing phenology - traits that are directly related to fitness and

115   typically measured in common gardens (Benito Garzón, Alía, Robson, & Zavala, 2011; Duputié

116   et al., 2015; Richardson et al., 2017; Valladares et al., 2014); (iii) as a consequence, predictions

117   of future species ranges are likely to be strongly influenced by the combined response of

118   different fitness-related traits to climate (Laughlin, 2018), but this structured combination of

119   intra-specific multi-trait variation defining species ranges has not been explored with empirical

120   data.

121   *Fagus sylvatica* L. (European beech, henceforth "beech") is a widely distributed

122   deciduous broadleaved temperate tree. In some parts of its range, beech has a late flushing

123   strategy to avoid late frosts, which has a generally detrimental effect on tree growth (Delpierre et

124   al., 2017; Gömöry & Paule, 2011; Robson, Rasztovits, Aphalo, Alia, & Aranda, 2013). Beech is

125   currently expanding at its northern distribution edge, whereas it experiences drought-induced

126   radial growth decline and increasing mortality at its southern edge (Farahat & Linderholm, 2018;

127   Stojnic et al., 2018). The extent to which this pattern will continue in the future depends on how

128   the combination of several fitness-related traits will influence the species' response to new

129   climates.

130   Here, we propose a new modeling approach that quantifies local adaptation and

131   phenotypic plasticity of four major phenotypic traits related to fitness (vertical and radial growth,

132   survival, and flushing phenology) and their interactions, to delimit species ranges under current

133   and future climates. To this purpose, we use the phenotypic measurements recorded in the

134   BeechCOSTe52 database (Robson, Benito Garzón, & BeechCOSTe52 database consortium,

135   2018), the largest network of common gardens for forest trees in Europe, covering virtually the

136   entire distribution range of the species. Our specific objectives are: (i) to quantify range-wide

137   patterns of phenotypic plasticity and local adaptation in growth, survival and flushing phenology;

138   (ii) to identify interactions among the different traits and the extent of their geographical

139   variation in local adaptation and phenotypic plasticity; (iii) to discuss how these fitness-related

140   traits delimit species ranges, and (iv) to better understand species ranges under new climate

141   scenarios and the role of trait variation in shaping the future species range.

142

143   **2. MATERIAL AND METHODS**

144   We calibrated two types of linear mixed-effect models using a combination of trait

145   measurements from common gardens where seeds coming from provenances from different

146   origins have been planted (provenances) and of environmental variables that we obtained for

147   these common gardens and provenances. The first model type (one-trait models) used single

148   traits as response variables and environmental data as explanatory variables. The second model

149   type (two-trait models) added a second trait as co-variate, which allowed the interaction of both

150   traits to be accounted for in the model. Finally, to quantitatively estimate the contribution of each

151   trait to explain beech range, we performed a binomial model using the occurrence of the species

152   as response variable (presence/absence) and the spatial predictions of all traits as explanatory

153   variables.

154

155   **2.1. Trait measurements**

156   We analyzed total tree height (vertical growth), diameter at breast height (DBH; radial growth),

157   survival and flushing phenology measured on a total of 153,711 individual beech trees that

158   originated from seeds collected from 205 populations (hereafter referred to as "provenances")

159   across Europe and planted at 38 common gardens (hereafter "trials") (Table 1; Supporting

160   Information Figure S1.1, Appendix S1). Briefly, the seeds were germinated in greenhouses and

161   planted in the trials at an age of two years. Plantations were carried out in two consecutive

162   campaigns, the first campaign (comprising 14 trials) in 1995 and the second one (comprising 24

163   trials) in 1998 (see more details in Robson et al., 2018). Survival was recorded as individual tree

164   survival. Leaf flushing was transformed from observational stage score data (qualitative

165   measurements that slightly differ among trials) to Julian days by adjusting flushing stages for

166   each tree with the Weibull function by trial (Robson et al., 2011, 2013).

167

168   **2.2. Environmental data**

169   We used the EuMedClim database that gathers climatic information from 1901 to 2014 gridded

170   at 1km (Fréjaville & Benito Garzón, 2018). The climate of the provenances was averaged for the

171   period from 1901 to 1990, with the rationale that the seeds planted in the common gardens

172   stemmed from trees growing during that period (Leites, Robinson, Rehfeldt, Marshall, &

173   Crookston, 2012). To characterize the climate of the common gardens, we calculated average

174   values for the period between the date of planting (either 1995 or 1998) and the year of

175   measurement of each trait for 21 climate variables (Supporting Information Table S1.1,

176   Appendix S1).In addition, we used the latitude and longitude of the provenance and of the trial as

177   proxies for the photoperiod and continentality, respectively (used in our flushing phenology

178   models).

179   Phenotypic predictions under future climates were performed using the representative

180   concentration   pathway   (RCP   8.5)   in   GISS-E2-R   from   WorldClim

181   (http://www.worldclim.org/cmip5_30s) for 2070. We deliberately chose only this pessimistic

182   scenario because for long-lived organisms such as forest trees it makes little difference whether

183   the projected situation will be reached in 2070 or some decades later.

184

185   **2.3. Statistical analysis**

186   2.3.1. Environmental variable selection

187   To avoid co-linearity and reduce the number of environmental variables to use in models, we

188   performed two principal component analyses (PCA), one for the climate variables related to the

189   provenance site and one for the climate variables related to the trial site. For tree height, DBH

190   and survival, we considered 21 variables for the provenance and 21 variables for the trial

191   (Supporting Information Figure S1.2, Appendix S1); whereas for leaf flushing, we only included

192   the temperature-related variables as well as latitude and longitude (a total of 20 variables),

193   because leaf flushing is known to be mainly driven by them (Basler & Körner, 2014).

194   The retained variables after the PCA screening were combined in models containing one

195   variable to characterize the climate of the provenance and one variable to characterize the

196   climate of the trial (Supporting Information Table S1.2, Appendix S1). We selected the

197   combination of environmental variables for each trait that minimize the AIC (Supporting

198   Information Table S1.2, Appendix S1).

199   2.3.2. One-trait and two-trait mixed-effect models

200   We used linear mixed-effect models to analyze the response of individual traits (one-trait

201   models) and the co-variation between two traits (two-trait models) to climate. We included the

202   climate at the provenance and the trial site as previously selected (Supplementary Table 1), the

203   age of trees, and for the leaf flushing model also latitude and longitude as fixed effects. The trial,

204   blocks nested within the trial and trees nested within block and trial, were included as random

205   effects to control for differences among sites and for repeated measurements of the same trees.

206   The random effect of the provenance was also included in the model. The common form of the

207   one-trait model was:

$$log\big(TR_{ijk}\big) = \alpha_0 + \alpha_1(Age_{ik}) + \alpha_2\big(CP_{ij}\big) + \alpha_3(CT_{ik}) + \alpha_4\big(CP_{ij}{}^2\big) + \alpha_5\big(CT_{ik}{}^2\big)$$

$$+ \alpha_6\big(Age_{ik} \times CP_{ij}\big) + \alpha_7(Age_{ik} \times CT_{ik}) + \alpha_8\big(CP_{ij} \times CT_{ik}\big) + \beta + \varepsilon$$

208   (Equation 1)

209   Where TR = trait response of the ith individual of the jth provenance in the kth trial; Age = tree age

210   of the ith individual in the kth trial; CP = climate at the provenance site of the ith individual of the

211   j^{th} provenance; CT = climate at the trial site of the ith individual in the kth trial; β = random effects

212   and ε = residuals. In addition, the model included the following interaction terms: Age and CP,

213   Age and CT, and CP and CT.

214   We analyzed trait co-variation across the species range by adding two specific traits of

215   interest in the same model. The common form of the two-trait model was:

216    $$log\big(TR_{ijk}\big) = \alpha_0 + \alpha_1(Age_{ik}) + \alpha_2\big(Cov_{ij}\big) + \alpha_3\big(CP_{ij}\big) + \alpha_4(CT_{ik}) + \alpha_5\big(Cov_{ik} \times CP_{ij}\big) +$$

217    $$\alpha_6(Cov_{ik} \times CT_{ik}) + \alpha_7(Cov_{ik} \times Age_{ik}) + \alpha_8\big(Age_{ik} \times CP_{ij}\big) + \alpha_9(Age_{ik} \times CT_{ik}) +$$

218    $$\alpha_{10}\big(CP_{ij} \times CT_{ik}\big) + \beta + \varepsilon$$

219   (Equation 2)

220   Where TR = trait response of the ith individual of the jth provenance in the kth trial; Age = tree age

221   of the ith individual in the kth trial; Cov = trait co-variate of the ith individual in the kth trial; CP =

222   climate at the provenance site of the ith individual of the jth provenance; CT = climate at the trial

223   site of the ith individual in the kth trial; β = random effects and ε = residuals. In addition, the

224   model included the following interaction terms: Cov and CP, Cov and CT, Cov and Age, Age

225   and CP, Age and CT, and CP and CT.

226   The one-trait and two-trait models for vertical and radial growth and leaf flushing were

227   fitted with the 'lmer' function, while the one-trait model for survival was fitted with the 'glmer'

228   function to accommodate logistic regressions (binomial family) in the analysis. We implemented

229   a stepwise-model procedure with four main steps to choose the best supported model (Akaike,

230   1992): (i) we fitted saturated models that included all the variables in the fixed part of the model;

231   (ii) we chose the optimal random component of the model by comparing the battery of models

232   using restricted maximum likelihood (REML), and selected the best model using the Akaike

233   information criterion (AIC) with criteria delta <2 (Mazerolle, 2006); (iii) we compared the

234   battery of models using maximum likelihood (ML) and selected the optimal fixed component

235   using the AIC criterion; (iv) we combined the best optimal random and fixed component

236   previously selected and adjusted them using REML to obtain the best performing model. All

237   model fits were done using the package 'lme4' (Bates et al., 2018).

238   For the best supported models, we visually analyzed the interactions of vertical growth,

239   radial growth, survival and leaf flushing with the environment (one-trait models) and between

240   traits (between the response and co-variate variable, i.e. the two-trait models). To do so, tree age

241   was fixed to 12 years for the radial and vertical growth and leaf flushing models and to 6 years

242   for the survival model. Mathematical interactions in one-trait models (CP x CT in equation 1)

243   represent the differences in trait values that can be attributed to the provenance (interpretable as

244   local adaptation) and those that can be attributed to the trial (interpretable as phenotypic

245   plasticity). Mathematical interactions in two-trait models (Cov x CT in equation 2) represent the

246   differences in trait values that can be attributed to a second trait that co-varies across the species

247   range with the first trait, mediated by the climate of the trial (representing phenotypic plasticity).

248   Unfortunately, survival could not be included in the two-trait models because there were

249   insufficient measurements shared with other traits in the same trials.

250   We estimated the percentage of the variance explained by the model attributed to the

251   fixed effects alone (marginal R^2) and attributed to the fixed and random effects together

252   (conditional R^2). We measured the generalization capacity (Pearson correlation) of the model

253   using cross-validation (64% of the data used for calibration and the remaining 34% for

254   validation).

255   2.3.3. Spatial predictions

256   We made spatial predictions for each trait across the species range for current and future climatic

257   conditions using the 'raster' package (Hijmans et al., 2017). For the prediction of current and

258   future trait variation, the climate variable for provenance was represented by the average climate

259   over the period from 1901 to 1990. The climate of the trial was set as the average climate from

260   2000 to 2014, for current trait predictions, and to 2070 for future predictions. For two-trait

261   models, the predicted values of the co-variate (DBH and leaf flushing) in the present were used

262   to estimate the predictions of vertical growth in the future. We calculated the spatial difference

263   between the future and the current conditions (future values minus current values) to illustrate

264   the amount of change that traits can accommodate. All spatial predictions of traits were delimited

265   within the distribution range of the species (EUFORGEN, 2009).

266   2.3.4. Quantification of the trait contribution to delimit the range of beech

267   We regressed the occurrence (presence/absence) of the species (EUFORGEN, 2009) against the

268   trait values obtained by the one-trait models using the 'glm' function to accommodate logistic

269   regressions (binomial family). The equation takes the form:

$$(RV) = \alpha_0 + \alpha_1(Vg) + \alpha_2(Rg) + \alpha_3(S) + \alpha_4(Lf) + \alpha_5(Vg \times S) + \alpha_6(Rg \times S) + \alpha_7(Lf \times S)$$
$$+ \alpha_8(Vg \times Rg) + \alpha_9(Vg \times Lf) + \alpha_{10}(Rg \times Lf) + \varepsilon$$

270   (Equation 3)

271   Where RV = presence/absence of beech; Vg = vertical growth; Rg = radial growth; S = survival;

272   Lf = leaf flushing; ε = residuals. In addition, the model included all possible pairwise linear

273   interactions of the included traits. The total deviance explained by the model was calculated

274   using the function 'Dsquared' of the package 'modEvA' (Barbosa, Brown, & Real, 2014). Then,

275   we performed an analysis of variance (ANOVA) of the model to obtain trait and trait interaction

276   deviances to estimate the percentage of the variance attributable to each trait.

277   All the models where performed with the R statistical framework version 3.2.0 (R Development

278   Core Team, 2015).

279

280   **3. RESULTS**

281

282   **3.1. Environmental variables selection**

283   The two PCA performed (provenance PCA and trial PCA) revealed two groups of variables, one

284   related with temperature and another more related with precipitation (Supporting Information

285   Figure S1.2, Appendix S1). The two most important axes of the provenance PCA explained

286   53.52 and 24.03% of the total variance, and those of the trial PCA explained 38.93 and 24.19%

287   (Supporting Information Figure S1.2, Appendix S1). We to retain the following variables for tree

288   growth and survival: BIO1, BIO5, BIO6, BIO12, BIO13, BIO14, Pet Mean and Pet Max. For the

289   leaf flushing models, we retained BIO1, BIO5, BIO6, MTdjf, MTmam, MTjja, Mtson, and

290   Mtdjfmam in addition to latitude and longitude.

291

292   **3.2. One-trait and two-trait models**

293   According to the best supported models (Table 2), the most important variable related to the

294   climate at the provenance for vertical growth, radial growth and survival was maximal potential

295   evapotranspiration (Pet Max). The most important variables related to climate at the trials were

296   precipitation of the wettest month (BIO13) for vertical growth, annual precipitation (BIO12) for

297   radial growth, and precipitation of the driest month (BIO14) for survival. In the case of leaf

298   flushing, the mean temperature of December, January and February (MTdjf) was the most

299   important climate variable for both the provenance and the trial site. The latitude of the

300   provenance and the trial and the longitude of the trial were also significant in the leaf flushing

301   model (see Supporting Information Table S1.3, Appendix S1 for detailed statistics on the

302   models). We observed significant interactions between the climate of the trial and that of the

303   provenance in all models (Table 2; Supporting Information Table S1.3, Appendix S1).

304   The capacity for generalization from the models (Pearson correlation coefficients) was high:

305   between 0.53 for radial growth and 0.73 for leaf flushing. The marginal R^2 ranged from 18% for

306   the survival model to 57% for the vertical growth model, while the conditional R^2 ranged from

307   40% for the survival model to 98% for the radial growth model (Supporting Information Table

308   S1.3, Appendix S1).

309

310   The significance of the fixed and random effects in the one-trait models was positively

311   affected (i.e., estimates were higher) by the addition of a second trait (Supporting Information

312   Table S1.4, Appendix S1). Furthermore, the co-variates and their interactions with the climate

313   variables of the trials were also significant in the two-trait models (Supporting Information Table

314   S1.4, Appendix S1). The capacity to generalize from the two-trait models was high: 0.76 for the

315   vertical growth-radial growth model and 0.77 for the vertical growth-leaf flushing model

316   (Supporting Information Table S1.4, Appendix S1). The marginal R^2 was 62% in the vertical

317   growth-radial growth model and 47% in the vertical growth-leaf flushing model, while the

318   conditional R^2 was 95% in the vertical growth-radial growth model and 99% in the vertical

319   growth-leaf flushing model (Supporting Information Table S1.4, Appendix S1).

320

321   **3.3. Spatial patterns of phenotypic trait variation from one-trait models**

322   Spatial predictions showed differences in phenotypic trait variation among traits (Figure 1, maps)

323   and the interaction graphs permitted the way that plasticity and local adaptation shape these

324   differences to be visualized (Figure 1, interaction graphs).

325   Vertical growth reached its maximum value at intermediate values of precipitation of the

326   wettest month in the trials (Figure 1a, interaction graph). These largest trees were predicted to

327   occur mostly over the northern and western part of the species range (Figure 1a, map). A signal

328   of local adaptation was detected in our models and is shown by the interaction graph, where each

329   line represents the response of provenances to high, intermediate and low levels of maximal

330   potential evapotranspiration.

331   Predicted radial growth across the species range presented a similar pattern to that of

332   vertical growth, with the lowest values in marginal populations, particularly at the southern

333   margin (Figure 1b, map). High annual precipitation coincided with high growth rates (Figure 1b

334   map), with a moderate signal of local adaptation in the form of some variation among

335   provenances (Figure 1b, interaction graph).

336   The lowest survival rates were predicted towards the east and at some isolated points in

337   the southernmost part of the range (Figure 1c, map). Survival increased towards those trials

338   where precipitation is high in the driest month, with weak local adaptation indicated by very

339   small –though statistically significant– differences among provenances (Figure 1c, interaction

340   graph).

341   Earlier flushing was predicted towards the south-eastern part of the range (Fig 1d, map),

342   with notable local adaptation indicated by large differences among provenances depending on

343   the latitude of origin (Figure 1d, interaction graph). Differences in flushing date among

344   provenances were particularly large in trials where the winter temperature is low (Figure 1d,

345   interaction graph).

346

347   **3.3. Patterns of phenotypic trait variation from two-trait models**

348   Overall, models with a second trait as co-variate produced different results to those considering a

349   single trait only. Predicted vertical growth was larger across the range when either radial growth

350   (Figure 2a) or leaf flushing (Figure 2b) was included as a co-variate. Vertical growth increased

351   with radial growth and precipitation (Figure 2a) and decreased in those regions where leaf

352   flushing was predicted to be late in the year (which corresponded mainly to the northern part of

353   the range) (Figure 2b).

354

355

356   **3.4. Spatial predictions of traits under climate change considering one- and two-trait**

357   **models**

358   Trait projections for 2070 showed an overall increase in tree growth, particularly for radial

359   growth (Figure 3a, b), but following similar spatial patterns to those predicted under current

360   conditions (Figure 1a, b). Tree survival was predicted to strongly decrease (with respect to that

361   predicted under current conditions, Figure 1c) in the east and throughout the range periphery,

362   while survival rates remained higher in the central part (Figure 3c). Leaf flushing showed similar

363   patterns to those predicted under current conditions (Figure 1d) but with an overall advance in

364   flushing dates (Figure 3d).

365   The prediction of vertical growth, considering radial growth as a covariate, showed an

366   overall increase across the distribution range (Figure 3e) with respect to the model projection of

367   vertical growth under future conditions (Figure 3a). This model showed differences in vertical

368   growth increase compared to the same model applied to current conditions (Figure 2a;

369   Supporting Information Figure S1.3e, Appendix S1). Predictions considering leaf flushing as a

370   co-variate tended to constrain vertical growth throughout the range (Figure 3f) compared with

371   the same model in current conditions (Figure 2b).

372

3.5. Total trait contribution to explain species ranges

All traits and their interactions significantly contributed to explain species occurrence (Table 3). The model explained 31% of the total deviance, with vertical growth accounting for 37%, radial growth for 33%, survival for 19%, and leaf flushing for 1%. The interaction between vertical growth and survival contributed with 3% to the total deviance, that between radial growth and leaf flushing with 2% and the remaining interactions with 1% or less (Table 3).

4. DISCUSSION

4.1. Contribution of phenotypic plasticity and local adaptation to range-wide variation in beech growth, survival and leaf flushing

Altogether, our results underpin that range-wide variation in fitness-related traits of beech is driven markedly more by phenotypic plasticity than by local adaptation (Supporting Information Table S1.3, Appendix S1). as happens in other species (Benito Garzón *et al*., *Under review*), and they imply that beech possesses a noteworthy capacity to respond to rapid climate change through acclimation. Although a short-term response through acclimation can be considered as positive for beech to keep pace with climate change, our results point out that the plastic component of tree growth and survival is mostly related to precipitation (Table 2), which follows highly unpredictable patterns (Pflug et al., 2018), making it difficult to evaluate whether acclimation will be enough for beeches to survive (but see our predictions for 2070 under RCP 8.5. showing an increase of mortality in young trees at the margins of the species ranges – Figure 3c). Local adaptation in tree growth (vertical and radial) and survival are driven by adaptation to

395   maximal potential evapotranspiration (Table 2), suggesting that populations are responding to

396   selection factors related to drought (Volaire, 2018). This is in agreement with the general

397   consensus that beech is a drought-sensitive species (Aranda et al., 2015), although there is

398   ongoing debate over the extent of resistance that beech has to drought (Pflug et al., 2018).

399   The plastic response of leaf flushing to climate was mainly driven by winter temperatures

400   (Table 2). There is a general consensus that these will increase globally in the future (Vautard et

401   al., 2014), and, accordingly, our projection for 2070 anticipates an advance in flushing through

402   most of the range (Figure 1d, 3d and S3d). However, leaf flushing can be constrained by local

403   adaptation to photoperiod (Gauzere et al., 2017; Way & Montgomery, 2015). The fact that

404   phenotypic plasticity and local adaptation in leaf flushing are driven by different environmental

405   parameters implies that these two processes would interact in the long-term. For instance,

406   phenotypic plasticity concerning winter temperatures might enhance local adaptation towards

407   new photoperiodical cues (i.e., shorter spring days), but the evolutionary time scale of local

408   adaptation makes this interaction very unlikely in the short-term.

409

4.2 Trait relationships across the species range

411   Trait inter-dependence varied to some extent along geographical gradients as the two-trait

412   models had higher predictive power and explained more variance than those based on a single

413   trait (Supporting Information Table S1.3 and Si1.4, Appendix S1). The tight albeit not perfect

414   positive interaction between tree vertical and radial growth (Figure 2a, interaction graph) is

415   unsurprising because of allometric relationships between these two variables, particularly in a

416   common-garden plantation that avoids competition among trees.

417   The biological basis of the observed co-variation between vertical growth and leaf

418   flushing is less obvious. One possible explanation is that vertical growth is greatly restricted by

419   late flushing in northern beech populations (Kollas, Körner, & Randin, 2014). This would also

420   explain our observation that the one-trait model predicts taller trees to occur in the North,

421   whereas the two-trait model predicts just the opposite. Interestingly, the two-trait model thus

422   implies that strong local adaptation of leaf flushing to photoperiod tends to constrain phenotypic

423   plasticity for vertical growth in northern beech populations (Way & Montgomery, 2015).

424

425   **4.3. Are spatial patterns of growth, survival and leaf flushing delimiting the range of**

426   **beech?**

427   Beech populations from certain eastern and southern parts of the distribution range seem most

428   sensitive to perturbation, as suggested by the lowest values for all traits considered (Figure 1).

429   Our analysis of species occurrence as a function of spatial trait values also suggests that a

430   combination of these traits contributes differently to the delimitation of the species range (Table

431   3), in particular: (i) mortality delimits certain parts of the southern and eastern range of beech,

432   reflecting the climatic marginality of the species in these areas, and meaning that these

433   populations are most threatened and making eastwards expansion of beech difficult (although

434   more studies on regeneration are needed to confirm this result); this is the case for many species

435   whose highest mortality is in the driest part of their range (Anderegg et al., 2015; Benito-Garzón

436   et al., 2013; Camarero, Gazol, Sancho-Benages, & Sangüesa-Barreda, 2015); (ii) the smallest

437   girths are predicted in the southern part of the distribution and the eastern part of the range,

438   suggesting that radial growth is mostly restricted by drought (interaction graph and map, Figure

439   1b), as has already been pointed out (Farahat & Linderholm, 2018); (iii) with very little variation

440   across climatic gradients, vertical growth alone will not delimit beech range. This is not the case

441   for other tree species, for which tree height is clearly delimiting species range (Chakraborty,

442   Schueler, Lexer, & Wang, 2018), highlighting the fact that no single best trait delimits tree

443   species ranges; (iv) projections of trees growing in southern and south-eastern regions that flush

444   early also have higher mortality and lower growth predictions than elsewhere within the species

445   range. However, when tree height and leaf flushing are pooled together in the two-trait model,

446   this leads to an decrease in vertical growth in the North; (v) it seems that in beech, and likely in

447   other species with local adaptation to photoperiod, phenology could restrict the northern

448   expansion of ranges (Duputié et al., 2015; Saltré, Duputié, Gaucherel, & Chuine, 2015), although

449   the link between phenology, survival and fitness is still unclear, and more experiments are

450   needed to better understand the interaction between photoperiod and phenology.

451

4.4. Implications of using trait approaches based on phenotypic variation to forecast beech

453   **sensitivity to climate change**

454   Overall, spatial patterns of vertical and radial growth, survival and leaf flushing predicted for the

455   future (Figure 3), are relatively similar to those predicted by the models under current conditions

456   (Figure 1 & 2), which is likely due to the high plasticity of these traits that allows populations to

457   respond to short-term changes in the environment. Our results, based on the study of phenotypic

458   variation, predict species persistence in the future (through high trait values) rather than

459   extinction and migration northwards as predicted by species distribution models based on the

460   occurrence of the species (Kramer et al., 2010; Stojnic et al., 2018).

461   Nevertheless, the direct comparison of our trait predictions for current and future

462   conditions allows us to detect some differences in their spatial patterns and total trait values

463   (Supporting Information Figure S1.3, Appendix S1), and gives us a better understanding of the

464   temporal dynamics of traits and their relative importance for beech persistence in the future. For

465   instance, our models of leaf flushing predict reduced geographical variability in phenology in the

466   future (from day 94 to 160 -Figure 1d- and from day 94 to 147 – Figure 3d-), as has been

467   reported worldwide (Ma, Huang, Hänninen, & Berninger, 2018). This is mostly explained by

468   larger advances in the phenology of populations at colder sites than those at warmer sites, likely

469   as a consequence of the larger increases in winter temperatures that happen in the North

470   (Kjellström et al., 2018). Survival of young trees is predicted to decrease at the margins of the

471   distribution, but less markedly than is predicted by species distribution models (Kramer et al.,

472   2010; Stojnic et al., 2018).

473   Including more than one trait related to growth likely reflects a conserved allometric

474   relationship between vertical and radial growth in the future (Figure 3e), but this may be a direct

475   consequence of the lack of competition among trees in our experimental design. Including

476   phenology in two-trait models seems to be detrimental for vertical growth, at least for northern

477   populations where growth is likely constrained by phenology (Figure 3f). However, our trait co-

478   variation approaches are limited to vertical growth as response variables, limiting our

479   understanding of the interplay that other traits can have across species range in the future.

480

481   **4.5. Limitations, perspectives and future research**

482   Although this study relied on the largest network of common gardens for a forest tree in Europe,

483   the resulting inferences suffer from a number of limitations. Our models are based in a limited

484   set of ages (from 2 to 15 years old). However, the expression of phenotypic plasticity changes

485   with age (Mitchell & Bakker, 2014), which can restrict the broad scope of our results to those

486   ages that we considered. This limitation is particularly pronounced for the case of survival (age

487   range 2 to 6 years), for which data only reflect early recruit survival. Other relevant proxies for

488   tree fitness as fecundity and reproduction have not been considered in our approach. In beech,

489   climate warming tends to increase seed production in northern populations (Drobyshev et al.,

490   2010) and to cause a decline in seedling density in southern ones (Barbeta, Peñuelas, Ogaya, &

491   Jump, 2011), which would be expected to continue under climate change.

492   Our predictions should help to shape future controlled experiments on those populations

493   most sensitive to climate (in the South – East of the range), and others designed to test those trait

494   relationships that are still unclear (phenology – growth – mortality) at the northernmost

495   distribution edge.

496

497   **REFERENCES**

498   Aitken, S. N., Yeaman, S., Holliday, J. A., Wang, T., & Curtis-Mclane, S. (2008). Adaptation , migration

499   or extirpation□: climate change outcomes for tree populations. *Evolutionary Applications*, (1), 95–

500   111. https://doi.org/10.1111/j.1752-4571.2007.00013.x

501   Akaike, H. (1992). Data analysis by statistical models. *No To Hattatsu*, *24*, 127–133.

502   Anderegg, W. R. L., Flint, A., Huang, C., Flint, L., Berry, J. A., Davis, F. W., … Field, C. B. (2015). Tree

503   mortality predicted from drought-induced vascular damage. *Nature Geoscience*, *8*, 367–371.

504   https://doi.org/10.1038/NGEO2400

505   Aranda, I., Cano, F. J., Gascó, A., Cochard, H., Nardini, A., Mancha, J. A., … Sánchez-Gómez, D.

506   (2015). Variation in photosynthetic performance and hydraulic architecture across European beech (

507   Fagus sylvatica L .) populations supports the case for local adaptation to water stress. *Tree*

508   *Physiology*, *35*(1), 34–46. https://doi.org/10.1093/treephys/tpu101

509   Barbeta, A., Peñuelas, J., Ogaya, R., & Jump, A. S. (2011). Reduced tree health and seedling production

510   in fragmented Fagus sylvatica forest patches in the Montseny Mountains (NE Spain). *Forest*

511   *Ecology and Management*, *261*(11), 2029–2037. https://doi.org/10.1016/j.foreco.2011.02.029

512   Barbosa, A. M., Brown, J. A., & Real, R. (2014). modEvA – an R package for model evaluation and

513   analysis. R package, version 0.1. Available at: http://modeva.r-forge.r-project.org/.

514   Basler, D., & Körner, C. (2014). Photoperiod and temperature responses of bud swelling and bud burst in

515   four temperate forest tree species. *Tree Physiology*, *34*(4), 377–388.

516   https://doi.org/10.1093/treephys/tpu021

517   Bates, D., Maechler, M., Bolker, B., Walker, S., Bojesen, R. H., Singmann, H., … Green, P. (2018).

518   lme4: Linear mixed-effects models using Eigen and S4. R package version 1.1-18-1. Available at:

519   http://CRAN.R-project. org/package=lme4.

520   Benito-Garzón, M., Ruiz-Benito, P., & Zavala, M. A. (2013). Interspecific differences in tree growth and

521   mortality responses to environmental drivers determine potential species distributional limits in

522   Iberian forests. *Global Ecology and Biogeography*, *22*(10), 1141–1151.

523   https://doi.org/10.1111/geb.12075

524   Benito Garzón, M., Alía, R., Robson, T. M., & Zavala, M. a. (2011). Intra-specific variability and

525   plasticity influence potential tree species distributions under climate change. *Global Ecology and*

526   *Biogeography*, *20*, 766–778. https://doi.org/10.1111/j.1466-8238.2010.00646.x

527   Benito Garzón, M., Gonzalez Munoz, N., Wigneron, J.-P., Moisy, C., Fernandez-Manjarres, J., & Delzon,

528   S. (2018). The legacy of water deficit on populations having experienced negative hydraulic safety

529   margin. *Global Ecology & Biogeography*, *27*, 346–356. https://doi.org/10.1111/geb.12701

530   Camarero, J. J., Gazol, A., Sancho-Benages, S., & Sangüesa-Barreda, G. (2015). Know your limits □?

531   Climate extremes impact the range of Scots pine in unexpected places. *Annals of Botany*, *116*, 917–

532   927. https://doi.org/10.1093/aob/mcv124

533   Chakraborty, D., Schueler, S., Lexer, M. J., & Wang, T. (2018). Genetic trials improve the transfer of

534   Douglas□fir distribution models across continents. *Ecography*, *41*, 1–14.

535   https://doi.org/10.1111/oik.02629

536   Delpierre, N., Guillemot, J., Dufrêne, E., Cecchini, S., & Nicolas, M. (2017). Tree phenological ranks

537   repeat from year to year and correlate with growth in temperate deciduous forests. *Agricultural and

538   Forest Meteorology*, *234–235*, 1–10. https://doi.org/10.1016/j.agrformet.2016.12.008

539   Des Roches, S., Post, D. M., Turley, N. E., Bailey, J. K., Hendry, A. P., Kinnison, M. T., … Palkovacs, E.

540   P. (2018). The ecological importance of intraspecific variation. *Nature Ecology & Evolution*, *2*(1),

541   57–64. https://doi.org/10.1038/s41559-017-0402-5

542   Doak, D. F., & Morris, W. F. (2010). Demographic compensation and tipping points in climate-induced

543   range shifts. *Nature*, *467*(7318), 959–962. https://doi.org/10.1038/nature09439

544   Drobyshev, I., Övergaard, R., Saygin, I., Niklasson, M., Hickler, T., Karlsson, M., & Sykes, M. T. (2010).

545   Masting behaviour and dendrochronology of European beech (Fagus sylvatica L.) in southern

546   Sweden. *Forest Ecology and Management*, *259*(11), 2160–2171.

547   https://doi.org/10.1016/j.foreco.2010.01.037

548   Duputié, A., Rutschmann, A., Ronce, O., & Chuine, I. (2015). Phenological plasticity will not help all

549   species adapt to climate change. *Global Change Biology*, *21*(8), 3062–3073.

550   https://doi.org/10.1111/gcb.12914

551   Enquist, B. J., Norberg, J., Bonser, S. P., Violle, C., Webb, C. T., Henderson, A., … Savage, V. M.

552   (2015). Scaling from Traits to Ecosystems: Developing a General Trait Driver Theory via

553   Integrating Trait-Based and Metabolic Scaling Theories. *Advances in Ecological Research*, *52*, 249–

554   318. https://doi.org/10.1016/bs.aecr.2015.02.001

555   EUFORGEN. (2009). Distribution map of Beech (Fagus sylvatica). Available at: www.euforgen.org.

556   Farahat, E., & Linderholm, H. W. (2018). Growth–climate relationship of European beech at its northern

557   distribution limit. *European Journal of Forest Research*, *137*(5), 1–11.

558   https://doi.org/10.1007/s10342-018-1129-9

559   Fréjaville, T., & Benito Garzón, M. (2018). The EuMedClim Database : Yearly Climate Data (1901 –

560   2014) of 1 km Resolution Grids for Europe and the Mediterranean Basin. *Frontiers in Ecology and*

561   *Evolution*, *6*, 1–5. https://doi.org/10.3389/fevo.2018.00031

562   Gauzere, J., Delzon, S., Davi, H., Bonhomme, M., Garcia de Cortazar-Atauri, I., & Chuine, I. (2017).

563   Integrating interactive effects of chilling and photoperiod in phenological process-based models. A

564   case study with two European tree species: Fagus sylvatica and Quercus petraea. *Agricultural and*

565   *Forest Meteorology*, *244–245*, 9–20. https://doi.org/10.1016/j.agrformet.2017.05.011

566   Gömöry, D., & Paule, L. (2011). Trade-off between height growth and spring flushing in common beech

567   (Fagus sylvatica L.). *Annals of Forest Science*, *68*(5), 975–984. https://doi.org/10.1007/s13595-011-

568   0103-1

569   Hijmans, R. J., Van Etten, J., Cheng, J., Mattiuzzi, M., Sumner, M., Greenberg, J. A., … Ghosh, A.

570   (2017). Package ' raster ': Geographic Data Analysis and Modeling. Available at: https://cran.r-

571   project.org/web/packages/raster/raster.pdf.

572   Kjellström, E., Nikulin, G., Strandberg, G., Christensen, O. B., Jacob, D., Keuler, K., … Vautard, R.

573   (2018). European climate change at global mean temperature increases of 1.5 and 2 degrees C above

574   pre-industrial conditions as simulated by the EURO-CORDEX regional climate models. *Earth*

575   *System Dynamics*, *9*(2), 459–478. https://doi.org/https://doi.org/10.3929/ethz-a-010180262 Rights

576   Kollas, C., Körner, C., & Randin, C. F. (2014). Spring frost and growing season length co-control the

577   cold range limits of broad-leaved trees. *Journal of Biogeography*, *41*(4), 773–783.

578   https://doi.org/10.1111/jbi.12238

579   Kramer, K., Degen, B., Buschbom, J., Hickler, T., Thuiller, W., Sykes, M. T., & de Winter, W. (2010).

580   Modelling exploration of the future of European beech (Fagus sylvatica L.) under climate change-

581   Range, abundance, genetic diversity and adaptive response. *Forest Ecology and Management*,

582   *259*(11), 2213–2222. https://doi.org/10.1016/j.foreco.2009.12.023

583   Laughlin, D. C. (2018). Rugged fitness landscapes and Darwinian demons in trait-based ecology. *New*

584   *Phytologist*, *217*, 501–503. https://doi.org/10.1111/nph.14908

585   Laughlin, D. C., & Messier, J. (2015). Fitness of multidimensional phenotypes in dynamic adaptive

586   landscapes. *Trends in Ecology & Evolution*, *30*(8), 487–496.

587   https://doi.org/10.1016/j.tree.2015.06.003

588   Leites, L. P., Robinson, A. P., Rehfeldt, G. E., Marshall, J. D., & Crookston, N. L. (2012). Height-growth

589   response to changes in climate differ among populations of interior Douglas-fir: a novel analysis of

590   provenance-test data. *Ecological Applications*, *22*(1), 154–165. https://doi.org/10.1890/11-0150.1

591   Ma, Q., Huang, J., Hänninen, H., & Berninger, F. (2018). Agricultural and Forest Meteorology Reduced

592   geographical variability in spring phenology of temperate trees with recent warming. *Agricultural*

593   *and Forest Meteorology*, *256–257*, 526–533. https://doi.org/10.1016/j.agrformet.2018.04.012

594   Mátyás, C. (1999). Forest genetics and sustainability. *Dordrecht, Boston: Kluwer Academic Publishers*.

595   https://doi.org/DOI: 10.1007/978-94-017-1576-8

596   Mazerolle, M. J. (2006). Improving data analysis in herpetology: Using Akaike's information criterion

597   (AIC) to assess the strength of biological hypotheses. *Amphibia Reptilia*, *27*(2), 169–180.

598   https://doi.org/10.1016/j.jclepro.2013.10.062

599   Mitchell, R. M., & Bakker, J. D. (2014). Intraspecific Trait Variation Driven by Plasticity and Ontogeny

600   in Hypochaeris radicata. *PLoS ONE*, *9*(10). https://doi.org/10.1371/journal.pone.0109870

601   Pedlar, J. H., & McKenney, D. W. (2017). Assessing the anticipated growth response of northern conifer

602   populations to a warming climate. *Scientific Reports*, *7*, 1–10. https://doi.org/10.1038/srep43881

603   Peterson, M. L., Doak, D. F., & Morris, W. F. (2018). Both life-history plasticity and local adaptation will

604   shape range-wide responses to climate warming in the tundra plant Silene acaulis. *Global Change*

605   *Biology*, *24*(4), 1614–1625. https://doi.org/10.1111/gcb.13990

606   Pflug, E. E., Buchmann, N., Siegwolf, R. T. W., Schaub, M., Rigling, A., & Arend, M. (2018). Resilient

607   Leaf Physiological Response of European Beech (Fagus sylvatica L.) to Summer Drought and

608   Drought Release. *Frontiers in Plant Science*, *9*, 187. https://doi.org/10.3389/fpls.2018.00187

609   R Development Core Team, R. (2015). R: A Language and Environment for Statistical Computing. R

610   Foundation for Statistical Computing, Vienna, Austria. Avaliable at: http://www.Rproject. org.

611   Reich, P. B., Sendall, K. M., Stefanski, A., Wei, X., Rich, R. L., & Montgomery, R. A. (2016). Boreal

612   and temperate trees show strong acclimation of respiration to warming. *Nature*, *531*, 633–636.

613   https://doi.org/10.1038/nature17142

614   Richardson, B. A., Chaney, L., Shaw, N. L., & Still, S. M. (2017). Will phenotypic plasticity affecting

615   flowering phenology keep pace with climate change? *Global Change Biology*, *23*(6), 2499–2508.

616   https://doi.org/10.1111/gcb.13532

617   Robson, M., Alia, R., Bozic, G., Clark, J., Forsteuter, M., Gomory, D., … von Wühlisch, G. (2011). The

618   timing of leaf flush in European beech (Fagus sylvatica L.) saplings. *Genetic Resources of European*

619   *Beech (Fagus Sylvatica L.) for Sustainable Forestry□: Proceedings of the COST E52 Final Meeting*

620   *. SERIE FORESTAL*, *22*, 61–80.

621   Robson, M., Benito Garzón, M., & BeechCOSTe52 database consortium. (2018). Data Descriptor□:

622   Phenotypic trait variation measured on European genetic trials of Fagus sylvatica L. *Scientific Data*,

623   *5*, 1–7. https://doi.org/10.1038/sdata.2018.149

624   Robson, M., Rasztovits, E., Aphalo, P. J., Alia, R., & Aranda, I. (2013). Flushing phenology and fitness

625   of European beech (Fagus sylvatica L.) provenances from a trial in La Rioja, Spain, segregate

626   according to their climate of origin. *Agricultural and Forest Meteorology*, *180*, 76–85.

627   https://doi.org/10.1016/j.agrformet.2013.05.008

628   Saltré, F., Duputié, A., Gaucherel, C., & Chuine, I. (2015). How climate, migration ability and habitat

629   fragmentation affect the projected future distribution of European beech. *Global Change Biology*,

630   *21*(2), 897–910. https://doi.org/10.1111/gcb.12771

631   Savolainen, O., Pyhäjärvi, T., & Knürr, T. (2007). Gene Flow and Local Adaptation in Trees. *Annual*

632   *Review of Ecology, Evolution, and Systematics*, *38*(1), 595–619.

633   https://doi.org/10.1146/annurev.ecolsys.38.091206.095646

634   Stahl, U., Reu, B., & Wirth, C. (2014). Predicting species' range limits from functional traits for the tree

635   flora of North America. *Proceedings of the National Academy of Sciences*, *111*(38), 13739–13744.

636   https://doi.org/10.1073/pnas.1300673111

637   Stojnic, S., Suchocka, M., Benito-Garzon, M., Torres-Ruiz, J., Cochard, H., Bolte, A., … Delzon, S.

638   (2018). Variation in xylem vulnerability to embolism in European beech from geographically

639   marginal populations Variation in xylem vulnerability to embolism in European beech from

640   geographically marginal populations. *Tree Physiology*, *38*, 173–185.

641   https://doi.org/10.1093/treephys/tpx128

642   Trumbore, S., Brando, P., & Hartmann, H. (2015). Forest health and global change. *Science*, *349*(6250),

643   814–818. https://doi.org/10.1126/science.aac6759

644   Urban, M. C., Bocedi, G., Hendry, A. P., Mihoub, J. B., Pe'er, G., Singer, A., … Travis, J. M. J. (2016).

645   Improving the forecast for biodiversity under climate change. *Science*, *353*(6304).

646   https://doi.org/10.1126/science.aad8466

647   Valladares, F., Matesanz, S., Guilhaumon, F., Araújo, M. B., Balaguer, L., Benito-Garzón, M., … Zavala,

648   M. A. (2014). The effects of phenotypic plasticity and local adaptation on forecasts of species range

649   shifts under climate change. *Ecology Letters*, *17*(11), 1351–1364. https://doi.org/10.1111/ele.12348

650   Vautard, R., Gobiet, A., Sobolowski, S., Kjellström, E., Stegehuis, A., Watkiss, P., … Jacob, D. (2014).

651   The European climate under a 2 ◦ C global warming. *Environmental Research Letters*, *9*, 1–11.

652   https://doi.org/10.1088/1748-9326/9/3/034006

653   Vitasse, Y., Lenz, A., Hoch, G., & Korner, C. (2014). Earlier leaf-out rather than difference in freezing

654   resistance puts juvenile trees at greater risk of damage than adult trees. *Journal of Ecology*, *102*,

655   981–988. https://doi.org/10.1111/1365-2745.12251

656   Volaire, F. (2018). A unified framework of plant adaptive strategies to drought: crossing scales and

657   disciplines. *Global Change Biology (in Press)*. https://doi.org/10.1111/ijlh.12426

658   Way, D. A., & Montgomery, R. A. (2015). Photoperiod constraints on tree phenology, performance and

659   migration in a warming world. *Plant, Cell & Environment*, *38*(9), 1725–1736.

660   https://doi.org/10.1111/pce.12431

661

662

663

664

DATA ACCESSIBILITY

666 All phenotypic data used in this study are available at

667 https://zenodo.org/record/1240931#.XBuSa81CeUk (Robson *et al.*, 2018). All the maps

668 generated in this study are available from the authors.

669

670

671

672

673

674

675

676

677

678

679

680

681

682

683

684   **Tables & Figures**

685   **Table 1.** The extent of data from the BeechCOSTe52 database used for modelling.

686   Measurements: total number of measurements; Trees: total number of individual trees; Trials:

687   total number of trials; Provenances: total number of provenances, Age: the age at which the trees

688   were measured. Columns indicate sample sizes for the traits: tree height (Height), diameter at

689   breast height (DBH), survival and leaf flushing that were used in the one-trait models, as well as

690   for the combined height-DBH, and height-leaf flushing records that were used in the two-trait

691   models.

692

	Height	DBH	Survival	Leaf flushing	H-DBH	H-Leaf flushing
Measurements	203 105	34 237	41 309	7 863	34 237	12 087
Trees	108 415	31 339	37 433	7 863	31 339	10 634
Trials	36	19	7	7	19	6
Provenances	205	186	114	62	186	150
Age	2 to 15	8 to 15	2 to 6	12	8 to 15	6, 9, 11, 12, 15

693

694

695

696

697

698

699

700 **Table 2.** Summary of the variables included in the final best-supported models (one- and two-

701 trait) for each trait analyzed. Environmental variables selected for the provenances and the trials

702 for the one-trait models of height, DBH, survival and flushing, and for the two-trait models of

703 height-DBH and height-leaf flushing. H: height; DBH: diameter at breast height; Lf: leaf

704 flushing; Pet Max: maximal monthly potential evapotranspiration; BIO12: annual precipitation;

705 BIO13: precipitation of wettest month; BIO14: precipitation of driest month; MTdjf: mean

706 temperature of December, January and February; Co-variate: trait covariate.

707

		one-trait models				two-trait models	
		Height	**DBH**	**Survival**	**Leaf flushing**	**H-DBH**	**H-Lf**
Variables	**Environment of the provenance**	Pet Max	Pet Max	Pet Max	MTdjf Latitude	Pet Max	Pet Max
	Environment of the trial	BIO13	BIO12	BIO14	MTdjf Latitude Longitude	BIO13	BIO13
	Co-variate					DBH	Lf

708

709

710

711

712

713

714

715 **Table 3.** Summary statistics for a generalized linear model (binomial family) of beech

716 occurrence (presence/absence) as a function of trait spatial predictions and their interactions.

717 Estimate: coefficient of the regression shown on a logarithmic scale; SE: standard error of fixed

718 variables; t: Wald statistical test that measures the point estimate divided by the estimate of its

719 standard error, assuming a Gaussian distribution of observations; p: p-value; DE: deviance

720 explained; Vg: vertical growth; Rg: radial growth; S: survival; Lf: leaf flushing.

|	**Estimate**	**SE**	**t**	**p**	**DE**
(Intercept)	-5.84	1.15e-02	-509.03	2.00E-16	
Vg	5.45	1.64e-02	332.93	2.00E-16	0.37
Rg	0.51	7.93e-03	64.67	2.00E-16	0.33
S	2.11	3.75e-03	562.83	2.00E-16	0.19
Lf	3.12	1.48e-02	210.94	2.00E-16	0.01
Vg x S	0.10	4.30e-03	21.08	2.00E-16	0.03
Rg x S	-0.60	2.04e-03	-295.94	2.00E-16	0.01
S x Lf	-1.40	4.02e-03	-348.1	2.00E-16	0.01
Vg x Rg	-1.11	4.62e-03	-240.58	2.00E-16	0.01
Vg x Lf	-7.81	2.15e-02	-363.18	2.00E-16	0.01
Rg x Lf	3.43	1.09e-02	313.89	2.00E-16	0.02
Model total deviance					**0.31**

721

722

723

724

725

726

727 **Fig 1.** Spatial projections for (a) vertical growth (cm), (b) radial growth (mm), (c) survival

728 (probability) and (d) leaf flushing (Julian days) generated using one-trait models (maps on the

729 left), and corresponding graphs of interactions between the best environmental predictor variable

730 across the trials divided according to environment at the provenance for each of the four traits

731 (graphs on the right). Black, dark grey, and light grey lines represent high, medium and low

732 values of the climatic variable of the provenances (as opposed to those of the trial, indicated on

733 the x-axis). The vertical lines represent the confidence intervals. The maps display the trait

734 projection for contemporary climate (inferred from 2000-2014 meteorological data) across the

735 current species range. The color gradient depicts the clinal variation from low (red) to high

736 (green) values of each trait. The values of the different traits are represented in the following

737 way: vertical growth (cm), radial growth (mm), probability of survival (0 =dead, 1=alive) and

738 leaf flushing (Julian days). Pet max prov: maximal monthly potential evapotranspiration at the

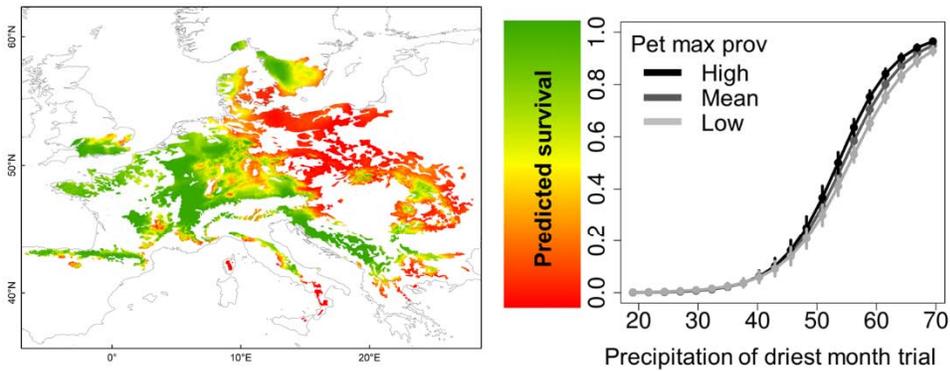739 provenance; Latitude prov: latitude of the provenance.
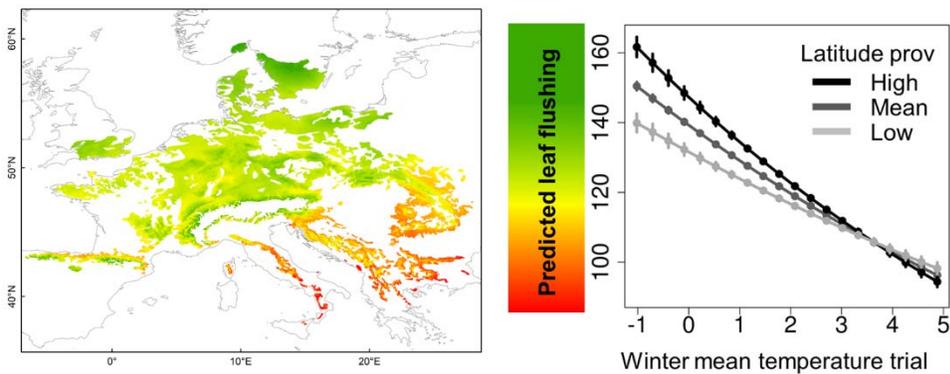
740

(a) Vertical growth
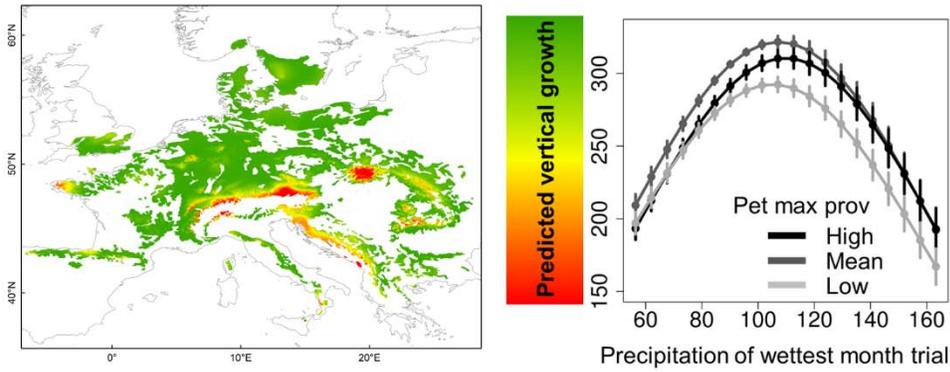
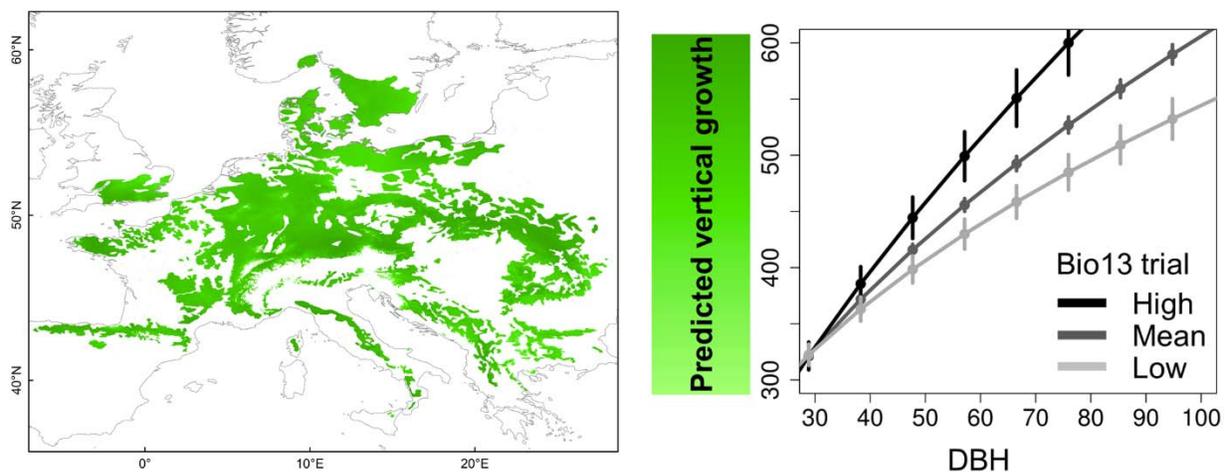## (b) Radial growth
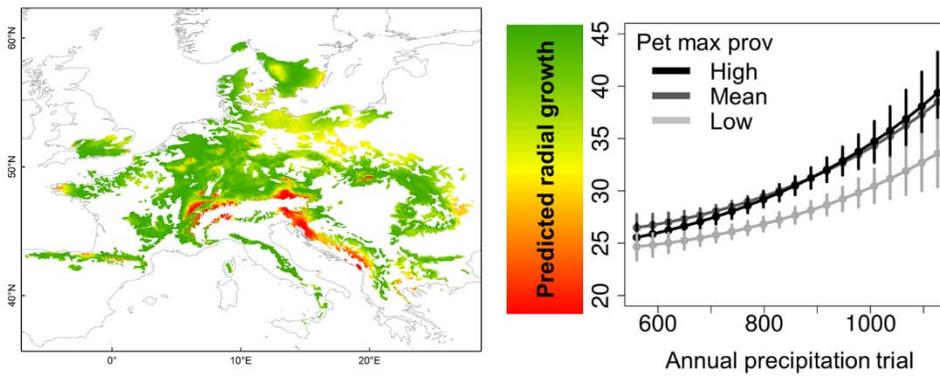
(c) Survival
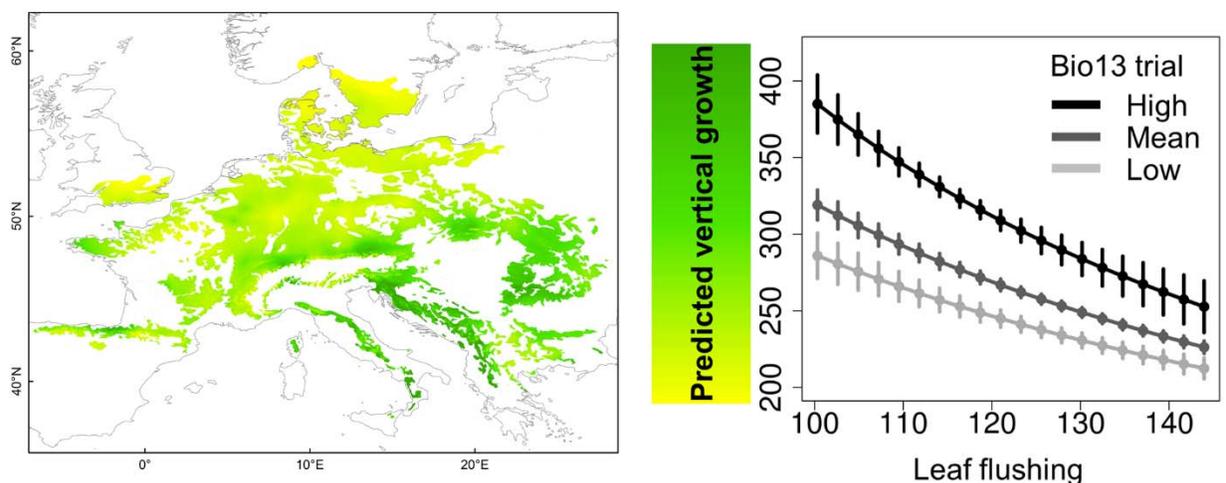

(d) Leaf flushing

741

742 **Fig 2.** Spatial projections of vertical growth (cm) for (a) Vertical-radial growth model and (b)

743 vertical growth-leaf flushing models (maps on the left), and the corresponding graphs of co-

744 variation between vertical growth and the covariate: (a) DBH (mm) and (b) leaf flushing (Julian

745 days). Black, dark grey, and light grey lines represent high, medium and low values of the

746 precipitation of the wettest month of the trial (BIO13). The vertical lines represent the

747 confidence intervals. The maps display the trait projection for contemporary climate (inferred

748 from 2000-2014 meteorological data) across the current species range. The color gradient depicts

749 the clinal variation in vertical growth from 200 cm (yellow) to 600 cm (green).
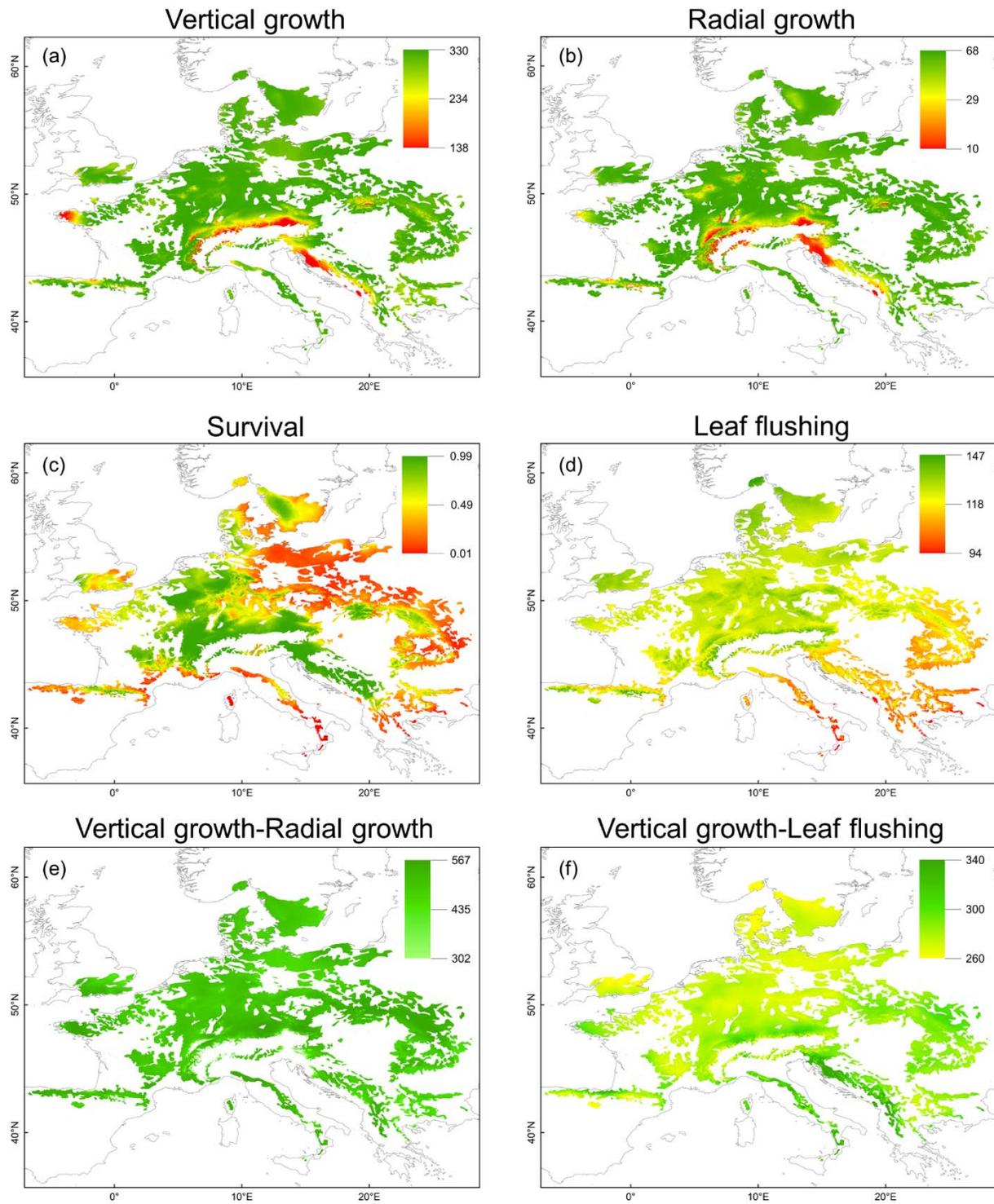

750

751   **Figure 3.** Spatial predictions for 2070 (RCP 8.5) across the species range for one-trait models:

752   (a) vertical growth (cm); (b) radial growth (mm); (c) probability of survival (0=dead; 1=alive);

753   (d) leaf flushing (Julian days); and for two-trait models: (e) vertical growth (cm; co-variate radial

754   growth) and (f) vertical growth (cm; co-variate leaf flushing). The color gradients depict the

755   clinal variation from low (red) to high (green) values.

756

757

758